Propagation of Excitation Pulses and Autocatalytic Fronts in Packed-Bed Reactors

Mads Kærn and Michael Menzinger*

Department of Chemistry, University of Toronto, Toronto, Ontario M5S 3H6 Canada

Received: September 17, 2001; In Final Form: January 14, 2002

We experimentally and numerically studied the velocity of excitation pulses in packed bed flow reactors as a function of the fluid flow velocity and the diameter of the glass beads used as packing material. Differential transport was absent. The downstream and upstream propagating pulses were observed to behave in a manner that is strikingly different from the simple Galilean translation expected in the case of an ideal homogeneous plug-flow. Downstream propagating pulses travel faster than anticipated, by a constant factor that depends on the bead size. Upstream propagating pulses travel at a lower velocity and become stationary above a critical value of the fluid flow velocity. Both the width and the intensity of up- and downstream propagating pulses increase when the fluid flow velocity is increased. Model calculations show that the accelerated downstream propagation and the decelerated upstream propagation agree qualitatively with enhanced turbulent diffusion within the packed bed. The formation of stationary pulses can be explained by the existence of a stationary fluid phase of stagnant pockets within the packed bed. Once excited, a stagnant pocket acts as a permanent super-critical perturbation, which causes excitation of the flowing medium and locks the temporal response in space. The dramatic increase of the pulse-intensity remains unexplained by the mentioned models.

1. Introduction

The diffusion-driven propagation of excitation pulses and of autocatalytic fronts has been a central theme in the study of spatially distributed active media for years.[1] The presence of convective transport adds new aspects to the problem. In practice, this arises most often in chemical engineering where packed bed reactors containing exothermic reactions have been studied both experimentally[2,3] and theoretically.[4,5] In recent years, there appeared in addition a number of theoretical studies of the effect of a flow on the propagation of excitation pulses. They focused on the effect of nonuniform flow profiles,[6−9] differential flows[10] and on the effects of hydrodynamics.[11−14] In this paper, we experimentally study the effect of a flow on the propagation of excitation pulses in a noncatalytic, isothermal packed bed reactor (PBR) where the interacting chemical species have identical transport coefficients.

One of the simplest flow systems used in theoretical investigations is the hypothetical, transversely uniform plug-flow reactor. It is described mathematically by a reaction−diffusion-advection (RDA) equation in one spatial dimension

$$\frac{\partial \boldsymbol{u}}{\partial t} = \boldsymbol{f}(\boldsymbol{u}) + \boldsymbol{D}\frac{\partial^2 \boldsymbol{u}}{\partial x^2} - \phi\frac{\partial \boldsymbol{u}}{\partial x} \tag{1}$$

The vector $\boldsymbol{u}$ contains the concentrations of the interacting chemical species, $\boldsymbol{f}(\boldsymbol{u})$ describes their interactions and ϕ, $\boldsymbol{D}$ are matrices whose diagonal elements are the flow and the diffusion coefficients. Although theoretical studies of eq 1 have made a number of predictions[15−17] that were subsequently verified experimentally,[18,19] real flow systems are rarely described by such simple equations. In practice, plug-flow conditions can be achieved, approximately, in a PBR, i.e., in a tube filled with an appropriate packing material such as glass-beads. The packing material establishes a more or less transversely uniform flow profile[19] by destroying the parabolic Poiseulle profile of the empty tube.

In the case where all the species flow at the same velocity ϕ and have identical diffusion coefficients D, as in the present study, eq 1 predicts that the flow simply translates a reaction−diffusion medium relative to the inflow boundary at $x = 0$ without changing its local properties. This can be shown mathematically by changing to the reference frame $z = x - \phi t$, which follows a given volume element as it is carried downstream by the flow. In this reference frame, eq 1 transforms into a reaction−diffusion equation

$$\frac{\partial \mathbf{u}}{\partial t} = \mathbf{f}(\mathbf{u}) + D\frac{\partial^2 \mathbf{u}}{\partial z^2} \tag{2}$$

In other words, the dynamics in the co-moving reference frame is the same as in a stationary reaction−diffusion system (equation 1 with $\phi = 0$). Suppose that the active medium in the absence of a flow supports the propagation of an autocatalytic front that moves with velocity c_0. The front could be the leading edge of an excitation pulse, a reaction front or the interface connection two steady states. Equation 1 then predicts that the effect of the flow is simple Galilean translation: the flow simply carries the reaction−diffusion medium downstream such that the velocity of the front relative to the inflow boundary is given by

$$c_{\mathrm{id}}{}^{\pm} = \phi \pm c_0 \tag{3}$$

The subscript id indicates that the velocity refers to the ideal plug-flow reactor described by eq 1. The velocity $c_{\mathrm{id}}{}^{+}$ is that of a reaction−diffusion front that propagates with the flow, whereas $c_{\mathrm{id}}{}^{-}$ is the velocity of a front that propagates against the flow. The velocity $c_{\mathrm{id}}{}^{+}$ is always positive (downstream propagation). The velocity $c_{\mathrm{id}}{}^{-}$ is negative (upstream propaga-

* To whom correspondence should be addressed. Phone & Fax: 416-978-6158. E-mail: mmenzing@chem.utoronto.ca.

10.1021/jp013541z CCC: $22.00
Published on Web 03/19/2002

tion) at sufficiently low flow velocities and positive at sufficiently high flow velocities. In both cases, the velocity increases linearly with the flow velocity and the proportionality factor is unity. The critical fluid flow velocity, ϕ_c, where the front is stationary ($c_{id}^- = 0$) corresponds to the situation where the upstream diffusion-driven propagation is exactly counterbalanced by the flow. This critical flow velocity is unique and equal to the reaction−diffusion velocity, $\phi_c = c_0$. In a bistable system, the critical flow velocity corresponds to the transition point between nonlinearly absolute ($\phi < \phi_c$) and nonlinearly convective ($\phi > \phi_c$) instability.[20]

To verify the theoretical predictions based on the ideal plug-flow reactor, we experimentally investigated the effect of a flow on the propagation of excitation pulses in a flow reactor that is usually modeled by eq 1; namely a noncatalytic, isothermal PBR where all the interacting species have equal flow and diffusion coefficients. The excitable medium was the Beluosov−Zhabotinsky (BZ) reaction. The experiments, which are described in sections 2 and 3, show that despite the simplicity of the experimental system, the propagation of excitation pulses is significantly different from what is predicted theoretically. The observed velocity, c^+, of pulses that propagate downstream with the flow is always considerably greater than the ideal velocity, $c^+ > c_{id}^+$. It is found to increase fairly linearly with the flow velocity, but the proportionality factor is as high as three compared to the value of one predicted within an ideal plug-flow reactor. On the other hand, the observed velocity, c^-, of the pulses that propagate against the flow is significantly less than the ideal velocity, $c^- < c_{id}^-$. The dependence of c^- on the flow velocity is nonlinear at low flow velocities and it decreases exponentially to zero as the flow velocity is increased. As expected, there is a critical fluid flow velocity, ϕ_c, where pulses become stationary. However, stationary pulses are observed over a very broad range of flow velocities and the critical flow velocity where the upstream propagation is balanced by the flow turns out not to be unique. Hence, the effect of the fluid flow is strongly anisotropic and it causes more than a simple Galilean translation in the downstream direction. Finally, it is observed that the intensity of both upstream and downstream propagating pulses is dramatically increased as the fluid flow velocity is increased.

In the theoretical section 4, we provide qualitative, physical explanations for these deviations from ideal behavior, based on minimal, dynamical models. An improvement of eq 1 is obtained by including turbulent mixing within the packed bed. This is done[21] by replacing the molecular diffusion coefficient with an empirical diffusion coefficient that reflects the increasing degree of turbulent mixing within the packed bed as the flow velocity increases. Inclusion of this enhanced diffusion within the packed bed accounts qualitatively for the increased ($c^+ > c_{id}^+$) and the decreased ($c^- < c_{id}^-$) velocities of downstream and upstream propagation. However, to account for the stationary pulses ($c^- = 0$) over a wide range of flow velocities, it is necessary and physically reasonable to include a stationary phase of stagnant pockets and what in the engineering literature is called particle-to-fluid mass transfer.[21] The idea is that the packed bed contains a stationary phase of stagnant pockets, such as boundary layers near the surface of the packing material, that interact diffusively with the mobile bulk phase. Simulations of this extended two-phase model show qualitative agreement with the experimental observations and suggest that the formation of stationary pulses can be understood in terms of a mechanism where a region of excited stagnant pockets acts as a constant excitatory perturbation that locks the temporal response of the flowing medium in space. This in turn indicates that the stationary pulses observed at high flow velocity reflect the high sensitivity of nonlinear chemical reactions to spatial inhomogeneities and imperfect mixing.[22−24] However, neither of the two models can account for the dramatic increase in intensity of pulses with increasing fluid flow velocity.

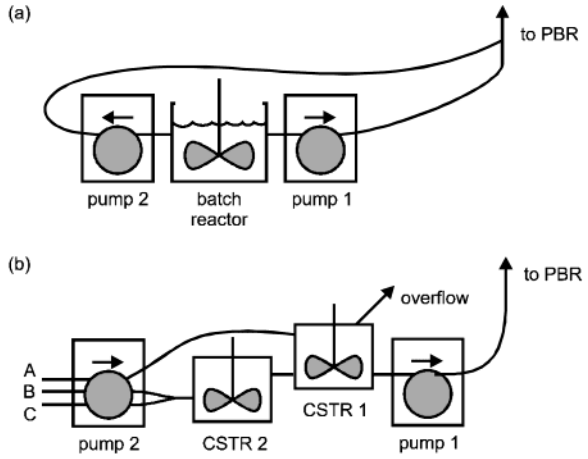

Figure 1. Experimental setups. PBR: packed-bed reactor, CSTR: continuously stirred tank reactor.

2. Experimental Section

The packed bed reactor, PBR, was a glass tube filled with glass beads. Tubes with inner diameters of 10 mm or 6.35 mm, and beads with diameters $d = 0.5$ or 1 mm were used. The PBR was illuminated from the back by two 20W fluorescent tubes. The propagation of excitation pulses was captured electronically using a black-and-white charge-coupled device (CCD) camera equipped with a 450−550 nm band-pass filter. This setup allows for the detection of the blue ferriin complex as white on a black background. In one experiment, we used a standard commercial digital camcorder to take color pictures of the reactor.

The PBR was fed BZ medium from below, using one of the two setups illustrated in Figure 1. The feeding configuration shown in Figure 1a was used in experiments where the pulse velocity was measured on a short time scale of less than 30 min. The one shown in Figure 1b was designed to maintain constant inflow conditions and a high excitation threshold at the reactor inlet over a longer time period. Experiments were carried out at a room temperature of 23±1 °C. The pulse velocity is sensitive to variation in temperature, and temperature variations are the main source of experimental error. For instance, the value of the reaction−diffusion velocity, c_0, was increased by about 12% when the temperature was raised from 23 °C to 25 °C.

In the configuration shown in Figure 1a, the PBR was fed reaction medium from an aerobic batch reactor using two peristaltic pumps, labeled pump 1 and pump 2. Pump 1 was a high precision pump (less than 2% error at a volumetric flow of 28.5 μL/min), whereas pump 2 was less precise but had high capacity. Pump 1 was used to control the flow velocity during an experiment, whereas pump 2 was used to rinse the PBR with BZ medium before an experiment and to remove CO_2 trapped between the glass beads between experiments. Applying a sufficiently fast fluid flow causes the glass beads to be suspended in the fluid, thus allowing for the release of gases entrapped between them. The bed of glass beads remained tightly packed at flow rates used in the experiments.

In the experiments that used the setup in Figure 1a, the BZ medium was prepared from analytic grade chemicals in the following way to obtain reproducible and well-defined conditions. First, 5 mL of a 0.025 M ferroin solution was added to a 10 mL solution prepared by mixing 5 mL 0.70 M H_2SO_4 and 5 mL 0.70 M $NaBrO_3$. This initially red solution turns blue shortly after mixing as ferroin is oxidized to ferriin. After one minute, 5 mL of a 0.10 M malonic acid solution and 5 mL water were added. This causes the system to return slowly to a state with a high ferroin concentration. This solution was incubated for 2 min before pumping it rapidly into the PBR using pump 2. The final composition of the medium was identical to that used in the investigation of excitation pulses in capillary tubes,[25] with the exception of a 2-fold decrease in the total catalyst concentration. After rinsing the PBR for about 2 min, the flow was stopped and an excitation pulse was initiated by inserting a silver-wire from the top into the glass-beads near the PBR outflow or into the feeding tubes. The silver-wire was removed as soon as the solution turned blue and the initial perturbation was allowed to develop into a propagating pulse before pump 1 was started.

Using a batch reactor to feed the PBR allows for constant conditions only over a limited time interval and spontaneous excitation at the reactor inflow occurred eventually in most of the realizations. Constant boundary conditions and suppression of spontaneous excitation were achieved by feeding the PBR from a continuously stirred tank reactor (CSTR) using the setup in Figure 1b. It consisted of two CSTR's coupled in series. The PBR was fed from CSTR 1 using Pump 1. CSTR 1 was in turn fed by two premixed feed-streams. One contained malonic acid, and the other contained a mixture of ferriin, sulfuric acid and bromate. The latter stream originated from a second CSTR 2 that was fed separate streams of stock solutions of ferroin ([ferroin] = 0.012 M) and acidified bromate free of bromine ($[BrO_3^-] = 0.30$ M, $[H_2SO_4] = 0.48$ M). The volumetric flow rates of the three feeds were set by pump 2 at 0.378, 0.364, and 0.369 mL/min for the feed-stream containing malonic acid, ferroin and sulfuric acid/bromate, respectively. The residence times of CSTR 1 and 2 were 209 and 270 s, respectively. The setting of pump 2 was always greater than that of pump 1 and excess fluid was removed from CSTR 1 through an overflow port. This port was also used to rinse and fill the PBR at the start of each experiment by connecting it directly to the PBR inlet.

3. Experimental Results

Representative space-time plots that show the propagation of the excitation pulses are given in Figure 2. The three plots show the radially averaged transmittance though a PBR packed with 1 mm beads at three different flow velocities: (a) no flow (reaction−diffusion system), (b) 0.55 cm/min, and (c) 1.1 cm/min. The experiments involved the experimental setup in Figure 1a. In Figure 2a, multiple pulses that propagate both upstream and downstream are emitted from the region where the first pulse was initiated with a silver-wire. These pulses propagate toward the reactor inlet at a velocity of $c^- = -c_0 = -0.24$ cm/min. At a distance of about 2.4 cm from the reactor inlet, the upstream pulse collides with a downstream (upward) propagating pulse that had formed spontaneously near the reactor inlet.

Figure 2b shows the slow upstream (downward) propagation of a pulse initiated near the reactor outlet and the rapid downstream (upward) propagation of a pulse that arose spontaneously near the reactor inlet, at a fluid flow velocity of 0.55 cm/min. It is clear that the flow causes the absolute velocity of the downstream pulse to increase and that of the upstream pulse to decrease, as one would expect from eq 3. Finally, the space-time plot in Figure 2c shows how the upstream oriented pulse becomes stationary ($c^- = 0$) when the flow velocity is increased further to 1.1 cm/min.

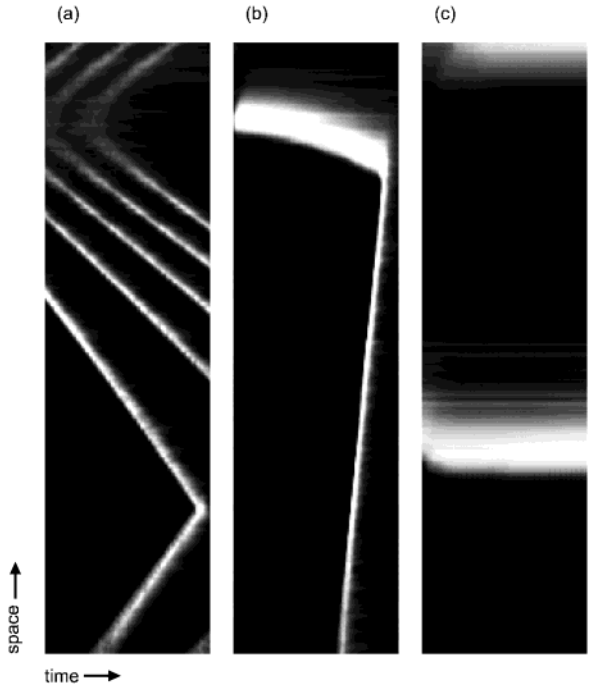

Figure 2. Space-time plots showing the propagation of excitation pulses over a time-period of 15 min (horizontal axis). 10 cm (vertical axis) of the reactor is shown. The flow is directed upward. The linear flow velocities are (a) 0 cm/min, (b) 0.55 cm/min and (c) 1.1 cm/min.

Contrary to what is expected for an ideal plug-flow reactor, it is observed that an increased fluid flow causes an increase in the width of the pulses as well as in the intensity of their blue phases. The increase in the width of the pulses is evident in Figure 2. The dramatic increase in intensity of the blue phase is not evident in Figure 2 due to the saturation of the CCD camera, but the increase in intensity is obvious and dramatic visually. The pulse is very faint and of a murky bluish color in the absence of a flow (Figure 2a). It is only detectable with high gain and offset on the CCD camera control unit. The blue phase of the pulse becomes strikingly more intense when the flow velocity is increased and the stationary pulse in Figure 2c is very bright blue. The four color-snapshots in Figure 3 show how the intensity of the blue phase of the upstream propagating pulses increases with the flow velocity. The pulse is barely visible in the absence of a flow (Figure 3a). The intensity increases gradually as the flow velocity is increased (Figure 3b and 3c) and the pulse is very bright in Figure 3d. A similar change in intensity is observed for downstream propagating pulses (not shown). Figure 3b−3d also indicate that there is a broadening of the blue phase along the wall of the reactor. This is consistent with an expected increase of the flow velocity due to the increased void fraction near the wall of the tube.[28]

Figure 4 shows the pulse velocity measured from space-time plots similar to those shown in Figure 2. Reactors packed with $d = 1$ mm (closed circles, subscript 1) and $d = 0.5$ mm (open circles, subscript 0.5) glass beads were used. The broken lines in Figure 4 show the dependences of the pulse velocity on flow velocity as predicted for an ideal plug-flow (equation 3) using the value of $c_0 = 0.24$ cm/min measured in the reactor with $d = 1$ mm beads.

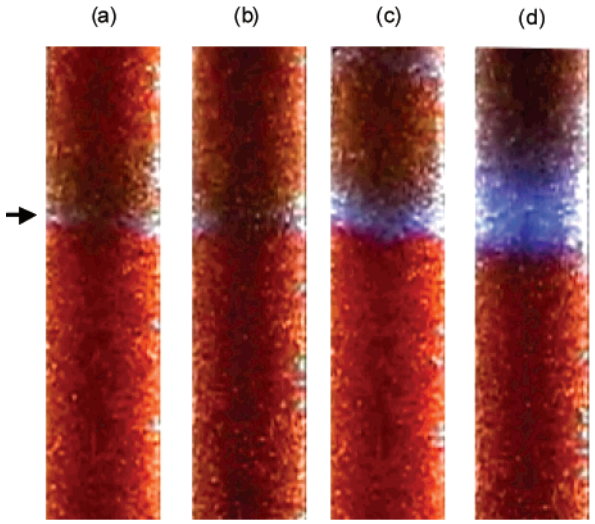

Figure 3. Color pictures of the PBR (6.35 mm ID, packed with 0.5 mm diameter beads) show the intensity of the excitation pulse at different flow velocities. An arrow indicates the location of the leading upstream (downward) oriented pulse. The volumetric flow rates are (a) no flow, (b) 28.5 μL/min, (c) 143 μL/min, and (d) 430 μL/min.

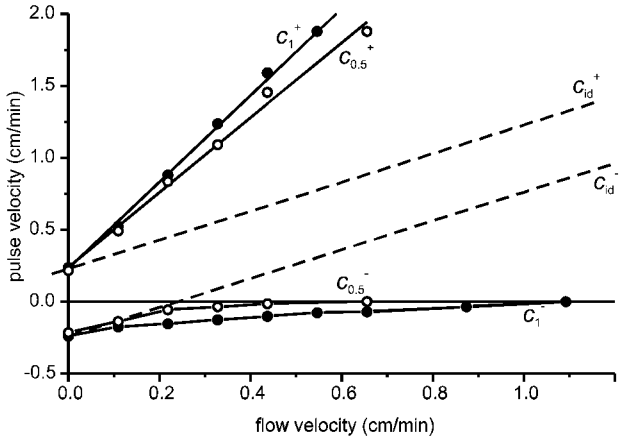

Figure 4. Velocities c^- and c^+ of up- and downstream propagating pulses in reactors packed with $d = 0.5$ mm (subscript 0.5) and $d = 1$ mm (subscript 1) glass-beads. The broken lines labeled $c_{id}^{\pm}$ show the velocities predicted by eq 3.

The propagation velocities are observed to be significantly different from what is expected in an ideal plug-flow reactor (equation 3). Although the dependence of pulse velocity $c(\phi)$ on flow velocity is fairly linear for the downstream propagating pulses (curves labeled c_1^+ and $c_{0.5}^+$ in Figure 4) the slopes of the curves are significantly greater than the theoretical prediction of unity. Linear regression gives slopes of 3.01 ± 0.06 and 2.6 ± 0.1 for the reactors packed with $d = 1$ and $d = 0.5$ mm beads, respectively.

For upstream propagating pulses the dependence of the pulse velocity on the fluid flow velocity also deviates significantly from eq 3. Instead of the predicted linear dependence, the absolute pulse velocity decreases to zero more or less exponentially and remains at zero as the flow velocity increases. Stationary pulses are observed when the flow velocity is above a certain critical value (see also Figure 2c and below). Note also that the size of the packing material has a significant effect on the propagation velocity since the absolute velocities, $|c^{\pm}|$, are consistently greater in the reactor packed with the larger beads.

The stationary pulses observed at high flow velocities were investigated further using the experimental setup illustrated in Figure 1b. With the feed-stream concentrations used in these experiments, the reaction−diffusion velocity c_0 was measured to be 0.16 cm/min in the 6.35 mm ID reactor packed with $d = 0.5$ mm beads. Figure 5 shows the space-time plot obtained in an experiment where the pump setting was increased by equal steps every 15 min. Initially, the flow velocity is about 0.12 cm/min (pump-setting (PS) 10) and the pulse propagates upstream. When the flow is then increased to $\phi = 0.24$ cm/min (PS 20), the pulse velocity decreases. The pulse becomes stationary after a short transient when the flow is increased further to $\phi = 0.36$ cm/min (PS 30). As the flow velocity is increased further to 0.48 cm/min (PS 40), the pulse is pushed a short distance downstream before it becomes again stationary. The same response is observed every time the flow velocity is further increased. Figure 5 shows that the stationary pulses persist when the flow velocity is 1 cm/min, but they may be observed even at $\phi = 2$ cm/min (not shown here). Note the pronounced increase of the pulse width with increasing flow velocity.

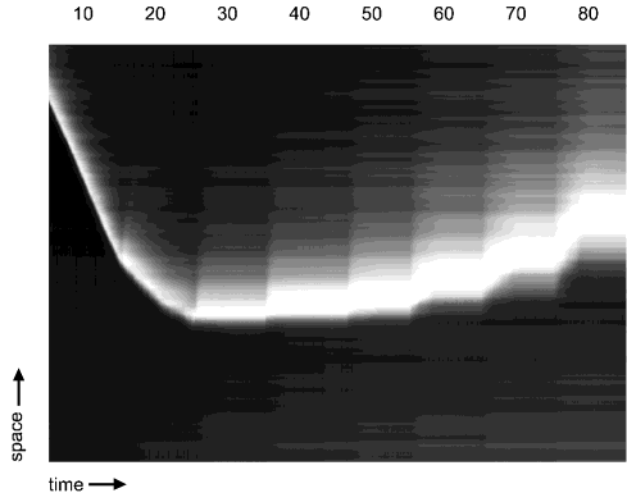

Figure 5. Space-time plot showing 4.3 cm of the PBR over a 2 h time period. The pump setting, indicated at the top of the figure, is increased by 10 units (about 0.12 cm/min) every 15 min. Stationary pulses are established after a short transient at flow velocities between 0.36 and 0.96 cm/min.

The space-time plots in Figure 6 provide clues about the mechanism of formation of stationary pulses. In Figure 6a, a motionless pulse was established at a flow rate of 0.53 cm/min. The flow velocity was then decreased to 0.06 cm/min and in response the pulse started to move steadily upstream. After 15 min, the flow velocity was restored to 0.53 cm/min and the pulse became motionless almost instantaneously at the new upstream location. This shows that the location of the stationary pulse is independent of the distance to the reactor inlet. Hence, it cannot be the result of an interaction with the constantly forced reactor inflow. Figure 6b shows the effect of first increasing and then decreasing the flow. Initially, a motionless pulse was established at a flow velocity of 0.72 cm/min. The flow rate was then increased to 1.5 cm/min and decreased to 0.53 cm/min 10 minutes later. The response of the increase in flow velocity is similar to what was observed in Figure 5: the pulse is initially pushed downstream before a stationary pulse is reestablished. Because a flow velocity of 0.53 cm/min is well above the value that allows for upstream propagation, it was expected that decreasing the flow velocity from 1.5 cm/min to 0.53 cm/min would have little or no effecton the location of

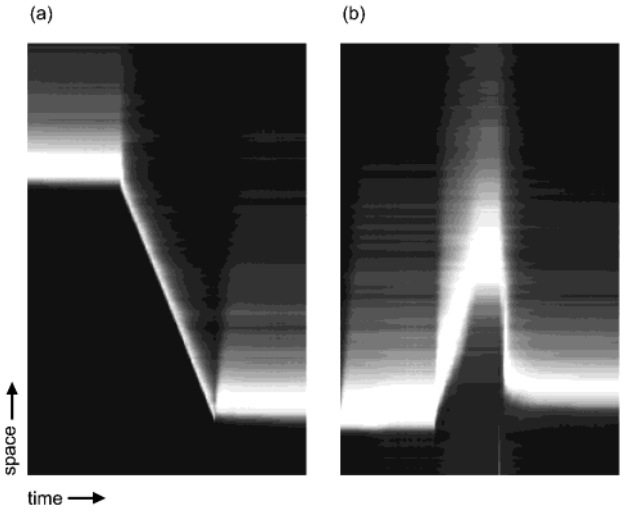

Figure 6. Space-time plots indicating (a) that the location of the stationary pulse is arbitrary and (b) that the packed bed contains stagnant pockets that remain excited when excitation pulse is pushed downstream.

the pulse. However, as seen in Figure 6b, lowering the flow velocity has a pronounced effect on the stationary pulse. A wide region upstream of the front is excited almost instantaneously when the flow velocity is decreased. It will be shown in section 4 that the excitation of the reactor bulk upstream of the pulse is the likely result of stagnant pockets within the packed bed that remain in the excited state after the pulse is pushed downstream.

4. Numerical Section

Numerical investigations were carried out using the two variable Rovinsky−Zhabotinsky model[26] of the ferroin-catalyzed BZ reaction. The kinetic terms $\boldsymbol{f}(\boldsymbol{u}) = f_1(u_1,u_2)$, $f_2(u_1,u_2)$ in equation. 1, which describe the evolution of the activator u_1 ([$HBrO_2$]) and the inhibitor u_2 ([ferriin]), are in this model given by

$$f_1 = \frac{1}{\epsilon}\left(u_1(1-u_1) - \left(2q\frac{\alpha u_2}{1-u2} + \beta\right)\frac{u_1-\gamma}{u_1+\gamma}\right), \qquad f_2 = u_1 - \frac{\alpha u_2}{1-u_2}, \quad (4)$$

where q, α, β, γ and ϵ are constants. Here, we take $q = 0.5$, $\alpha = 0.1$, $\beta = 0.0034$, $\gamma = 0.001$, and $\epsilon = 0.1$. For these parameter values, the model system has a stable steady state with a relatively low excitability threshold.

4a. Effects of Turbulent Diffusion. As mentioned in the Introduction, in chemical engineering the effect of hydrodynamics in packed bed reactors is frequently modeled by assuming that a turbulent flow increases the effective diffusion coefficient. The empirical expression for effective diffusion coefficient is often written[21] as a sum of molecular and turbulent diffusion terms

$$D(\phi,d) = a'D_0 + b'd\phi, \quad (5)$$

where D_0 is the molecular diffusion coefficient, d is the diameter of the glass beads and a', b' are constants. This expression is found to be valid at Reynolds numbers greater than 5.[21] The flow velocities used in the experiments lie in the range between 0 and 2 cm/min and the Reynolds numbers are much less than unity. Injecting a pulse of tracer and observing it disperse would

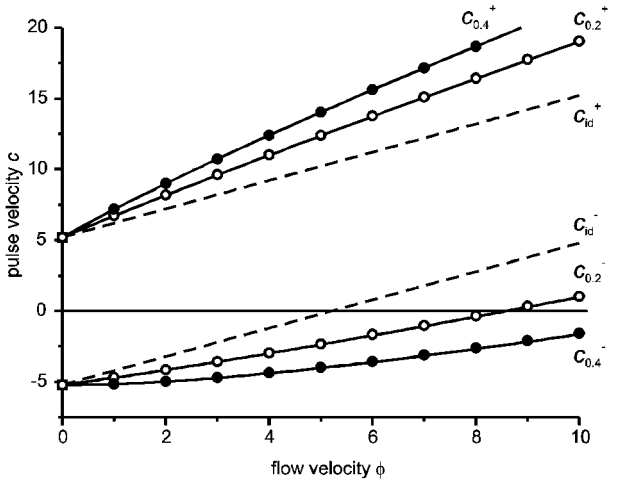

Figure 7. Calculated pulse velocities for the diffusion coefficient given by eqs 6, 7. Broken lines correspond to constant (molecular) diffusion, $a = a'D_0 = 1$, $b = b'd_p = 0$. Closed and open circles are obtained for $a = 1$, $b = 0.2$, and $a = 1$, $b = 0.4$, respectively. Full lines are obtained from the Fisher equation augmented with a flow term (equation 7).

allow for an improved approximation for the effect of the flow and bead size on axial dispersion. Even though eq 5 may not give quantitative agreement with the experimental observations, it can still provide a qualitative explanation for the observation that the absolute velocity of both up- and downstream propagating pulses is higher than predicted for an ideal plug-flow reactor.

Figure 7 shows the dependence of the pulse velocities on the flow velocity in numerical simulations where molecular diffusion is replaced by the flow dependent diffusion coefficient in eq 7 with $a = a'D_0 = 1$. Simulations where done for $b = b'd = 0$ (broken lines in Figure 7), $b = 0.2$ (open circles) and $b = 0.4$ (closed circles). Note that the full lines are actually obtained analytically from the one-variable Fisher-flow equation given by

$$\frac{\partial u_1}{\partial t} = ku_1(1-u_1) + (a+b\phi)\frac{\partial^2 u_1}{\partial x^2} - \phi\frac{\partial u_1}{\partial x} \quad (6)$$

Equation 6 corresponds to the equation for u_1 in the RZ model (eq 4) with α and β equal to zero and $k = 1/\epsilon$. The propagating front is in this case the interface connecting the unstable state at $u_1 = 0$ to the stable state at $u_1 = 1$. The minimum front velocities for the up- and downstream propagating fronts, denoted $c_b^{\pm}$, are obtained using the method described by Murray[27] as

$$c_b^{\pm} = \phi \pm 2\sqrt{k(a+b\phi)}. \quad (7)$$

The full lines in Figure 7 are obtained using $b = 0$ (broken lines), $b = 0.2$ ($c_{0.2}^{\pm}$) or $b = 0.4$ ($c_{0.4}^{\pm}$) and $k = 6.7852$, $a = 1$. The excellent agreement with the 2-variable RZ model (open and full circles) shows that the Fisher equation captures exactly the motion of the front.

Replacing the molecular diffusion coefficient with the turbulent diffusion coefficient in eq 5 can account qualitatively for a number of experimental observations. As observed in the experiments (Figure 4), the absolute pulse velocity, $|c_b^{\pm}|$ is higher than predicted for an ideal plug-flow reactor (eq 3, broken lines) and it increases with bead size, i.e., with parameter b. Furthermore, the dependence of the pulse velocity on the flow velocity is fairly linear, which was also observed in Figure 4 for the downstream propagating pulses. Finally, as observed

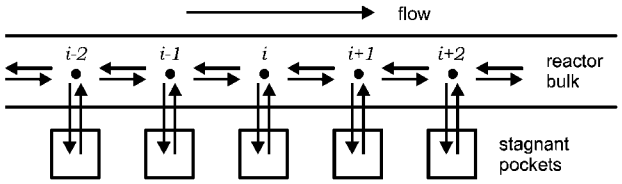

Figure 8. Two-phase model of a PBR with a mobile phase of flowing medium and a stationary phase of stagnant pockets.

in Figures 2, 3, and 5 the width of the pulse increases with flow velocity (not shown).

Although turbulent diffusion can account qualitatively for some of the experimental observations, it fails to give the correct dependence of the pulse velocity on the flow velocity for the upstream travelling waves. Because diffusion is an isotropic process, replacing the molecular diffusion coefficient with a flow-dependent diffusion coefficient, be it the simple functional form in eq 5 or one that is estimated experimentally, cannot account for the strongly anisotropic effect of the flow observed in Figure 4. Also, the models in eqs 4 and 6 predict a stationary pulse only at a unique flow velocity ϕ_c (see Figure 7 and eq 7). Flow-dependent diffusion cannot capture the formation of stationary pulses over a wide range of flow velocities (Figure 5) or the increase in intensity (Figure 3) when the flow velocity is increased.

4b. Effects of a Stationary Phase. The stationary pulses observed at high flow velocities may be accounted for if the reactor bed contains a stationary phase of stagnant fluid pockets. This is a reasonable assumption from the point of view of hydrodynamics. In a Pouiselle flow, which arises in an empty tube (see e.g., ref 15), the flow profile is parabolic and the flow velocity is zero at the wall of the reactor. Similarly, in a PBR, it is reasonable to expect that in the packed bed there are boundary layers near the reactor walls and near the surface of the particles used as packing material where the flow velocity is zero. The interaction between the bulk of the reactor and the particle surface is in the engineering literature called the particle-to-fluid mass transfer.[21] Although a quantitative modeling of the radial inhomogenities in the flow velocity is a rather complicated task (see e.g., ref 28), some of the qualitative features may be captured by assuming that the PBR contains a mobile and a stationary phase that interacts diffusively with each other.

The two-phase model is illustrated in Figure 8. The length of the reactor is divided into N spatial points separated by the distance Δx. The dynamics at a distance $x_i = i\Delta x$ from the inlet is determined by the equations

$$\frac{d\boldsymbol{u}_i}{dt} = \boldsymbol{f}(\boldsymbol{u}_i) + D\Delta x^{-2}(\boldsymbol{u}_{i-1} + \boldsymbol{u}_{i+1} - 2\,\boldsymbol{u}_i) - 0.5\phi\,\Delta x^{-1}(\boldsymbol{u}_{i-1} - \boldsymbol{u}_{i+1}) + \delta(\boldsymbol{u}_i^p - \boldsymbol{u}_i), \quad (8)$$

$$\frac{d\boldsymbol{u}_i^p}{dt} = \boldsymbol{f}(\boldsymbol{u}_i^p) - \delta\rho(\boldsymbol{u}_i^p - \boldsymbol{u}_i), \quad (9)$$

where $\boldsymbol{u}$ is the concentration vector for the flowing bulk, $\boldsymbol{u}^p$ is the vector containing the concentrations in the stationary, stagnant pockets, δ is the particle-to-surface mass transfer coefficient[21] and ρ is the ratio of the bulk volume to the volume of the stagnant pockets. Setting δ equal to zero in eq 8 can be used to mimic the special case where the mobile phase is unaffected by the dynamics within the stagnant pockets (see Figure 10b below). The stagnant pockets occupy in the simulations 1% of the free reactor volume ($\rho = 99$). Zero-flux conditions are imposed at $i = 0$ and at $i = N$. The simulations use the two-variable RZ model in eq 4 to describe the local kinetics, $\boldsymbol{f}(\boldsymbol{u}_i)$ and $\boldsymbol{f}(\boldsymbol{u}_i^p)$, and the diffusion coefficient is taken to be constant and equal to unity. Allowing for turbulent diffusion does not qualitatively affect the results.

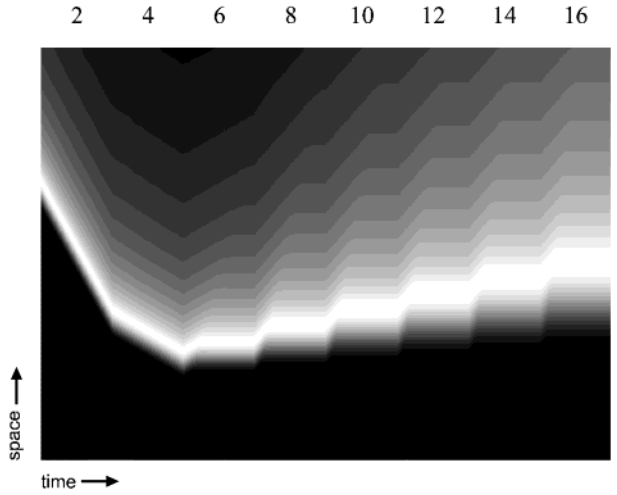

Figure 9. Space-time plot, obtained in a simulation that mimics the experiment in Figure 5. The flow velocity is increased by factors of 2 at regular time-intervals (10 time-units). The pulse becomes stationary when the flow velocity is greater than about 5. The values of δ and ρ are 0.05 and 99, respectively. Other parameter values are the same as in Figure 7. The reactor-length is 100 units.

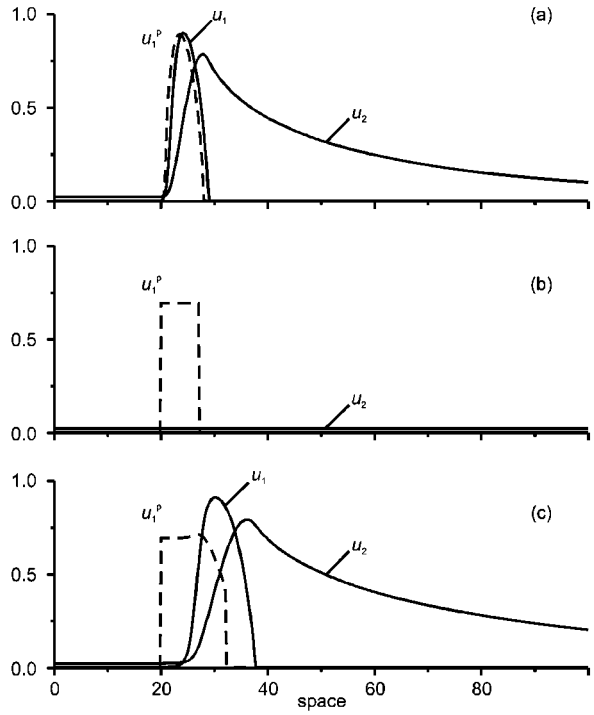

Figure 10. Spatial profiles of the variables u_1, u_2, and u_1^p. Panel (a) shows an upstream propagating pulse at $\phi = 4$. Panel (b) shows how a number of stagnant pockets remain in the excited state when the reactor bulk returns to the stable, unexcited steady state. Panel (c) shows the re-excitation of the bulk by the excited stagnant pockets and the formation of a stationary pulse at $\phi = 8$.

Figure 9 shows the result of a simulation that mimics the experiment in Figure 5, where the flow velocity was increased in steps at regular intervals. In the simulation, the flow velocity is low ($\phi = 2$) during the first time-interval (10 time-units) and

a pulse propagates upstream. The velocity of the pulse decreases when the flow velocity is doubled to $\phi = 4$. It becomes stationary when the flow velocity is increased to $\phi = 6$. Everytime the flow is increased further, the pulse is pushed a short distance downstream before it becomes again stationary. This is the same behavior as that observed in Figure 5. Note also how the width of the stationary pulse increases when the flow velocity is increased, in excellent agreement with the experimental observations.

The stationary pulses observed in Figure 9 can be explained qualitatively by a mechanism by which stagnant pockets that are in the excited state cause excitation of the medium in the mobile phase. Three steps are involved: (1) excitation of the stagnant pockets at low flow velocity by the passage of an upstream propagating pulse, (2) a sustained excitation within the stagnant pockets at high flow velocity where the pulse in the mobile phase is pushed downstream, and (3) excitation of the medium in the mobile phase by stagnant pockets in the excited state. These three steps are illustrated in Figure 10. In Figure 10a, the flow velocity is low ($\phi = 4$) and the pulse (full lines) moves to the left. The excited portion of the pulse where u_1 is high causes excitation (broken line) of the stagnant pockets. Once a stagnant pocket is excited, it may remain in the excited state even after the medium in the mobile phase has returned to the unexcited, stable steady state. This is illustrated in Figure 10b. In simulation, the profile in Figure 10a was taken as the initial condition for of u^p_1 and u^p_2, whereas the value of u_1 and u_2 are kept fixed in the stable steady state. After transients have died out, a number of pockets that were initially located within the zone of high autocatalyst levels in the bulk (Figure 10a) remain the excited state. The bulk-interaction term in eq 9 makes the kinetics similar to that in a continuously stirred tank reactor, and causes the local kinetics to change from excitable to bistable. Given the appropriate initial and parameter conditions, a stagnant pocket may thus remain excited indefinitely.

In the simulation in Figure 10b, the bulk of the reactor is returned to the stable steady state instantaneously and is forced to remain in this state by setting the transfer coefficient δ equal to zero in eq 8. If the value of δ is kept at $\delta = 0.05$, then the perturbation provided by the excited pockets excites the bulk and causes the formation of an upstream propagating pulse (not shown). Figure 10c shows the effect on the pulse in Figure 10a of increasing the flow velocity from $\phi = 4$ to $\phi = 8$. In the absence of stagnant pockets (Figure 7) or when the mobile phase is unaffected by the stagnant pockets (Figure 10b), the pulse is pushed downstream and eventually out of the system. In the presence of stagnant pockets and a sufficient particle-to-surface mass transfer, however, the pulse is only pushed a short distance downstream before the stationary profile shown in Figure 10c is established.

The experiment in Figure 6a, which showed that a pulse could become stationary at any location within the reactor, is consistent with the two-phase model in Figure 8. The location where the pulse becomes stationary is in the model determined by the location of the excited pocket that is closest to the reactor inlet. In other words, it depends on the location of the pulse at the moment at which the flow velocity is increased above the critical value. The experiment in Figure 6b is also in excellent agreement with the two-phase model. It is clear from that figure that excitation occurs within the region where the pulse was located 4 to 10 min earlier, which can readily be accounted for by the presence of stagnant pockets that remain in the excited state after the pulse was pushed downstream.

5. Discussion

We have presented an experimental investigation of the effect of a fluid flow on excitation pulses in a noncatalytic, isothermal packed bed flow reactor where all the interacting species have identical flow and diffusion coefficients. The experimental system is to the first approximation described by "plug-flow" reaction−diffusion−advection (RDA) equations,[4,30] which are often used in the theoretical investigations of flow systems. We find that the effects of the fluid flow on the velocity, the width and the intensity of the pulses are significantly different from the simple Galilean translation predicted by such equations. While the velocity of downstream propagating pulses increases more or less linearly with the flow velocity, the proportionality factor is three times higher than predicted based on Galilean translation. On the other hand, the velocity of upstream propagating pulses depends nonlinearly on flow velocity and is significantly lower than predicted theoretically. The absolute value of the pulse velocity decreases to zero as the flow velocity increases and a stationary pulse is observed over a very broad range of flow velocities. The acceleration of downstream propagating pulses and the deceleration of upstream propagating pulses can be accounted for qualitatively by including flow-enhanced axial dispersion due to turbulent mixing within the packed bed. This turbulent diffusion can also account for the observation that the width of a pulse increases when the flow velocity is increased. We have used a particularly simple functional form (eq 5) for the dependence of the diffusion coefficient $D(\phi;d)$ on the flow velocity ϕ and diameter of the packing material d. A more quantitative expression for $D(\phi;d)$ may give better quantitative agreement between model and experiments. However, the effect of the flow is strongly anisotropic and the up- and downstream propagating pulses are affected differently by the fluid flow. Diffusion is an isotropic process and a more quantitative model of how the flow enhances the effective diffusion coefficient would not be able to explain fully the experimental observations.

The appearance of stationary pulses over a wide range of flow velocities can be accounted for qualitatively by including a stationary phase of stagnant pockets within the packed bed that interacts diffusively with the bulk phase of the flowing fluid. On the basis of a simple two-phase model, which shows good qualitative agreement with experimental observations, we suggest that the appearance of stationary pulses at high flow velocities is due to a mechanism where stagnant pockets in the excited state act as a permanent super-critical perturbation that causes excitation of the medium in the mobile phase and locks the temporal response of the medium in space. The mechanism works in the following way: consider first the response of an external perturbation that is applied at a distance x_0 from the inflow boundary. The characteristic response time of the medium, for instance the time it takes before maximal intensity is reached or the duration of the pulse, is given by τ. The response length ξ, for instance the width of the pulse, depends on the flow velocity because the flow distributes the temporal response of the medium in space. It is given by $\xi = \phi\tau$ in the kinematic limit where the effect of diffusion is neglected. The presence of excited stagnant pockets is equivalent to the presence of a permanent external perturbation. This constant forcing locks the temporal evolution of the medium in space and gives rise to a stationary structure, much in the same way as we have demonstrated elsewhere for oscillatory media.[19,29] Note that the presence of stagnant pockets only affects pulses that are oriented against the flow and only at fluid flow velocities greater than a critical value.

The present results—acceleration of excitation pulses through faster-than-molecular diffusion, and the arrest of upstream propagating pulses through interaction with the boundary layers surrounding the particles that make up the packing material—were obtained for an excitable medium in a packed bed reactor without differential transport. The propagation of an excitation pulse is driven by the propagation of its autocatalytic reaction-front. As a result, the observations reported here should be directly transferable to both isothermal and exothermic autocatalytic reactions. Although it is well established[4,30] that turbulent diffusion affects the propagation of reaction fronts in packed bed reactors with exothermic reactions and differential transport, it remains to be seen to what extent the effects reported here occur in these reactors.

Although extending the standard RDA equations by including turbulent diffusion $D(\phi;d)$ within the packed bed and a stationary phase of stagnant pockets provides a qualitative mechanistic explanation for the experimental observations, there are a number of observations that cannot be accounted for by these simple models. First of all, the fluid flow has a significant anisotropic effect even at low flow velocities. This cannot be accounted for by modeling the flow-dependent mixing $D(\phi;d)$ with the packed bed as an isotropic diffusive process or by including a stationary phase of stagnant pockets. Furthermore, the experiment reproduced in the color Figure 3 demonstrates a dramatic increase of the intensity of the pulse, i.e., of the blue color which reflects the ratio, [ferriin]/[ferroin], of the oxidized to reduced forms of the BZ catalyst, as the fluid flow velocity is increased. Neither the inclusion of turbulent diffusion, nor the inclusion of stationary stagnant pockets succeeded in even approximately duplicating this increase in productivity (i.e., in the extent of the oxidation reaction). A satisfactory explanation of this interesting phenomenon is still lacking. It may be related to the increased rate of autocatalytic reactions due to imperfect mixing.[22−24]

The prospect that the productivity of packed bed flow reactors might be increased by the inadvertent or deliberate incorporation of imperfections and of poorly mixed regions may have important applications in applied science and engineering.

Acknowledgment. This work was performed with support from the NSERC of Canada and from the Danish Research Academy.

References and Notes

(1) Michailov, A. S. *Foundations of Synergetics I*; Springer-Verlag: New York, 1990.
(2) Puszynski, J.; Hlavacek, V. *Chem Eng. Sci.* **1984**, *39*, 681.
(3) Sheintuch, M.; Adjaye, J. *Chem. Eng. Sci.* **1990**, *45*, 1897.
(4) Sheintuch, M.; Shvartsman, S. *AIChE J.* **1996**, *42*, 1062.
(5) Yakhnin, V. Z.; Menzinger, M. *Chem. Eng. Sci.* **1995**, *50*, 2853.
(6) Doering, C. R.; Horsthemke, W. *Phys. Lett. A.* **1993**, *182*, 227.
(7) Allen, M. A.; Brindley, J.; Merkin, J. H.; Pilling, M. J. *Phys. Rev. E* **1996**, *54*, 2140.
(8) Biktashev, V. N.; Holden, A. V.; Tsyganov, M. A.; Brindley, J.; Hill, N. A. *Phys. Rev. Lett.* **1998**, *81*, 2815.
(9) Biktashev, V. N.; Biktasheva, I. V.; Holden, A. V.; Tsyganov, M. A.; Brindley, J.; Hill, N. A. *Phys. Rev. E* **1999**, *60*, 1897.
(10) Rovinsky, A. B.; Zhabotinsky, A. M.; Epstein, I. R. *Phys. Rev. E* **1998**, *58*, 5541.
(11) Diewald, M.; Matthiessen, K.; Muller, S. C. *Phys. Rev. Lett.* **1996**, *77*, 4466.
(12) Legawiec, B.; Kawczynski, A. L. *J. Phys. Chem. A* **1997**, *101*, 8063.
(13) Cliffe, K. A.; Tavener, S. J.; Wilke, H. *Phys. Fluids* **1998**, *10*, 730.
(14) Perez-Villar, V.; Munuzuri, A. P.; Perez-Munuzuri, V. *Phys. Rev. E* **2000**, *61*, 3771.
(15) Rovinsky, A. B.; Menzinger, M. *Phys. Rev. Lett.* **1992**, *69*, 1193.
(16) Kuznetsov, S. P.; Mosekilde, E.; Dewel, G.; Borckmans, P. *J. Chem. Phys.* **1997**, *106*, 7609.
(17) Andrésen, P.; Bache, M.; Mosekilde, E.; Dewel, G.; Borckmans, P. *Phys. Rev. E.* **1999**, *60*, 297.
(18) Rovinsky, A. B.; Menzinger, M. *Phys. Rev. Lett.* **1993**, *70*, 778.
(19) Kærn, M.; Menzinger, M. *Phys. Rev. E.* **1999**, *60*, 3471.
(20) Chomaz, J. M. *Phys. Rev. Lett.* **1992**, *69*, 1931.
(21) Wakao, N.; Kaguei, S. *Heat and Mass Transfer in Packed Beds*; Gordon and Breach Science Publishers: New York, 1982.
(22) Epstein, I. R. *Nature* **1995**, *374*, 321.
(23) Strizhak, P.; Menzinger, M. *J. Phys. Chem.* **1996**, *100*, 19 182.
(24) Strizhak, P.; Ali, F.; Menzinger, M. *J. Am. Chem. Soc.* **1998**, *120*, 1343.
(25) Toth, A.; Showalter, K. *J. Phys. Chem.* **1995**, *99*, 2058.
(26) Rovinsky, A. B.; Zhabotinsky, A. M. *J. Phys. Chem.* **1984**, *88*, 6081.
(27) Murray, J. D. *Mathematical Biology*; Springer-Verlag: New York, 1993.
(28) Bey, O.; Eigenberger, G. *Chem. Eng. Sci.* **1997**, *52*, 1365.
(29) Kærn, M.; Menzinger, M. *Phys. Rev. E.* **2000**, *61*, 3335; Kærn, M.; Menzinger, M. *Phys. Rev. E.* **2000**, *62*, 2994; Kærn, M.; Menzinger, M. *J. Phys. Chem. A* **2001**, *00*, 00.
(30) Froment, G. F.; Bischoff, K. B. *Chemical Reactor Analysis and Design*; J. Wiley & Sons: New York, 1990.